A&A 477, 165–172 (2008)
DOI: 10.1051/0004-6361:20078525

Astronomy & Astrophysics

Tidal radii and masses of open clusters⋆

A. E. Piskunov[1,2,3], E. Schilbach[1], N. V. Kharchenko[1,3,4], S. Röser[1], and R.-D. Scholz[3]

[1] Astronomisches Rechen-Institut, Mönchhofstraße 12-14, 69120 Heidelberg, Germany
e-mail: [apiskunov;elena;nkhar;roeser]@ari.uni-heidelberg.de
[2] Institute of Astronomy of the Russian Acad. Sci., 48 Pyatnitskaya Str., 109017 Moscow, Russia
e-mail: piskunov@inasan.rssi.ru
[3] Astrophysikalisches Institut Potsdam, An der Sternwarte 16, 14482 Potsdam, Germany
e-mail: [apiskunov;nkharchenko;rdscholz]@aip.de
[4] Main Astronomical Observatory, 27 Academica Zabolotnogo Str., 03680 Kiev, Ukraine
e-mail: nkhar@mao.kiev.ua

Received 22 August 2007 / Accepted 9 October 2007

ABSTRACT

Context. In a previous paper we obtained King's parameters for 236 of 650 Galactic open clusters identified in the ASCC-2.5.
Aims. Estimating tidal radii by use of observable parameters available for all clusters. Bias-free results are required.
Methods. We use methods of stellar statistics and develop a semi-empirical model of open clusters.
Results. We check two effects impacting the determination of tidal radii from a fitting of King's profiles to the observed density distribution, i.e., ellipticity of open clusters and a bias depending on distances. Though a typical cluster has an elliptical form, the effect is rather weak to produce a prominent bias in the resulting tidal radii. In contrast, a distance dependent bias is not negligible and can cause a systematic underestimation of tidal radii computed with ASCC-2.5 data by a factor of two for the most distant clusters of our sample. This finding is used to correct the original results for 236 clusters and to extend the system of tidal radii and masses to all 650 clusters. We found that the semi-major axis of the projected distribution of cluster members on the sky is a parameter suited to estimate tidal radii of open clusters of our sample. No systematic differences are found between measured and calibrated tidal radii. From the comparison with mass estimates based on star counts and on the assumption of the Salpeter IMF, empirical evidence is obtained for an evolution of cluster mass functions starting in young clusters.
Conclusions. The set of homogeneous parameters available for all clusters of our sample is extended by tidal radius and mass. Within 850 pc where our sample is complete, the distributions of tidal radii and masses peak at $r_t \approx 6$ pc and $\log M_c/m_\odot \approx 2.5$, respectively. In young open clusters, the mass distributions show differences to the Salpeter IMF, and this discrepancy increases with cluster age.

Key words. Galaxy: open clusters and associations: general – solar neighborhood – Galaxy: stellar content

1. Introduction

Our current project aims at studying the properties of the local population of Galactic open clusters. The basic sample consists of 641 open clusters and 9 compact associations identified in the all-sky compiled catalogue ASCC-2.5 (Kharchenko 2001). For each cluster, we determined membership (Kharchenko et al. 2004) and derived a homogeneous set of cluster parameters (Kharchenko et al. 2005a,b). The sample is found to be complete up to a distance of about 850 pc from the Sun (Piskunov et al. 2006). This completeness limit corresponds to a distance modulus ($V - M_V$) of about 10−10.5 (Schilbach et al. 2006) in the case of our cluster sample. In our latest paper of this series (Piskunov et al. 2007, hereafter called Paper I), we present tidal radii and masses of 236 open clusters from this sample. The tidal radii are determined from fitting three-parametric King's profiles to the observed integrated density distribution. Compared to a few open clusters with tidal parameters already available, the number looks very high. However, this subsample can not be used for a statistical study of the population of open clusters, mainly, due to its incompleteness. In this paper we try to fill this gap by constructing a consistent set of tidal parameters for the complete sample.

In an ideal case, all 650 clusters should be passing through the "King's profile fitting pipeline" which we developed in Paper I. Nevertheless, due to the low quality of density profiles of the remaining clusters, this is not possible, and we had to look for another approach. The idea is to use the 236 clusters as standards to find a relation between tidal radius and an observable parameter available for all clusters. This approach assumes that standard parameters are free of biases as much as possible.

The paper has the following structure. In Sect. 2 we briefly describe the input data and the basic terminology widely used in the present work. In Sect. 3 we consider possible biases which may be inherent in our determination of tidal radii. Section 4 is devoted to building up the homogeneous system of tidal radii and masses for the complete cluster sample. In Sect. 5 we describe the properties of this sample of tidal parameters and compare tidal masses with counted masses available from the literature. In Sect. 6 we summarize the results.

⋆ The determined tidal radii and masses for 650 clusters are listed in a table that is available in electronic form at the CDS via anonymous ftp to cdsarc.u-strasbg.fr (130.79.128.5) or via http://cdsweb.u-strasbg.fr/cgi-bin/qcat?J/A+A/477/165

2. Data and terminology

In this paper we use the results of the previous work based on the study of 650 nearby open clusters identified in the ASCC-2.5. For a better understanding, we briefly describe the most relevant aspects and designations widely used in the following sections.

In each cluster, membership determination is carried out in an iterative process that takes into account spatial (projected density profile), photometric (color magnitude diagram, CMD), and proper motion (vector point diagram, VPD) distributions of stars within a cluster area. As a result, we obtain new coordinates of the cluster centre, the cluster size, location of the cluster's main sequence (MS) in the CMD, and the mean proper motion of the cluster. The data are used to derive the distance of the cluster, reddening, and age (Kharchenko et al. 2005a,b). At the end of the iterations, each star gets membership probabilities $P_{\rm ph}$, and P_μ of its belonging to the cluster which are calculated from the location of the star in the CMD and VPD relative to the cluster MS and the mean proper motion, respectively (see Kharchenko et al. 2004). Stars deviating from the reference values, both in CMD and VPD, by less than one rms error are considered to be the most probable members, and we call them 1σ-members. Those deviating by less than two rms errors are called 2σ-members, by less than three rms errors – 3σ-members. For convenience, we call all stars in the cluster area "4σ"-members. Consequently, the 1σ-members form a subsample of the 2σ-members that are, in turn, a subsample of the 3σ-members, and so on. Depending on the desired application, which may require either a cleaner or more complete selection of cluster members, the suitable subsample is chosen, e.g. all cluster parameters were determined using data on 1σ-members. The results are included in the catalogue of open cluster data (COCD) and its extension (Kharchenko et al. 2005a,b).

The cluster size was evaluated by analyzing the projected density profiles of stars in the wider neighbourhood of the cluster centre. In accordance with the general rule, the apparent cluster radius r_2 is the maximum angular distance from the cluster centre where 1σ-members could be still found. Since for each cluster the distance from the Sun was determined, the radius r_2 can be easily expressed in linear units (pc). This parameter is obtained for all 650 clusters (for more details on structural properties of open clusters see Schilbach et al. 2006). In contrast, the tidal radius is derived from the fitting of King (1962) density profiles to the observed integrated density distribution for 236 clusters of the sample (Paper I). Assuming that the obtained King parameters are related to the limiting radii of open clusters, we compute tidal masses for 236 clusters. In order to stress their empirical origin, we call these parameters, hereafter, measured tidal radii $r_{\rm t}^{\rm m}$, and measured tidal masses $M_{\rm c}^{\rm m}$.

3. Biases in measured tidal radii

3.1. Correction for the membership sample

For the majority of 236 clusters, we obtained several sets of King's parameters, depending on the membership group used. In this case, the solution with the best goodness-of-fit is chosen. However, comparing the tidal radii computed with different membership groups, we found small but systematic differences in the solutions (see Table 1 in Paper I). On average, the solutions based on samples with less certain membership provide slightly smaller tidal radii. This effect can probably be explained by a less reliable estimation of the background in the solutions with 2σ-, 3σ-, and "4σ"-groups than with the 1σ-sample.

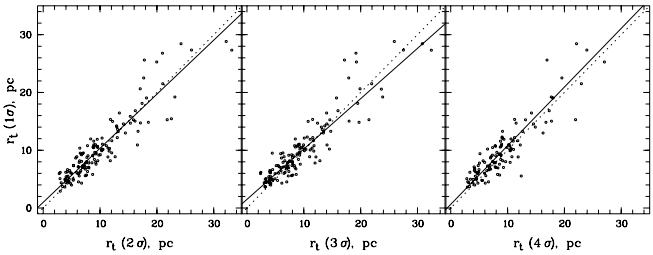

Fig. 1. Relations between the tidal radii computed with 2σ- (*left*), 3σ- (*middle*), "4σ"- (*right*) membership groups and with the 1σ-sample. In each panel, the corresponding least square fit is shown by a solid line. The dotted lines are the loci of equal radii.

In order to obtain all the tidal radii in the system of 1σ-members, we compare 2σ-, 3σ-, and "4σ"-solutions with the corresponding tidal radius based on the 1σ-sample, for each membership group separately. We consider only those clusters for which we obtained at least two sets of King's parameters that are larger than their rms errors, i.e. from the membership group under test and from the 1σ-sample. The corresponding relations are fitted by regression lines and are shown in Fig. 1. The results are used in Sect. 4 to convert the tidal radii obtained from the solutions with 2σ-, 3σ-, and "4σ"-membership groups into the system defined by the 1σ-members.

3.2. Cluster ellipticity

There are several reasons forcing a cluster to get a non-spherical shape, e.g., the galactic tidal field (Wielen 1974, 1985), differential rotation of the Galaxy, encounters with giant molecular clouds (Gieles et al. 2006). Nevertheless, it is still unclear whether an ellipsoidal form can be assumed to be one of the general properties of open clusters. In the past, indications of a flattening were obtained only for a small number of selected clusters. Raboud & Mermilliod (1998a,b) and Adams et al. (2001, 2002) found evidence of flattening in the Pleiades and in Preasepe. Their results support the predictions of Wielen's model that explains the ellipsoidal form of clusters by tidal coupling with the Galaxy. On the contrary, flattening found in the Hyades (Oort 1979) deviates from theoretical expectations. Recently, Chen et al. (2004) determined the ellipticity of 31 open clusters, residing in the Galactic anticentre direction, from stellar counts in the 2MASS. Since they do not publish orientations of ellipses in space, a comparison of their data with theoretical predictions is not possible.

As the information on the ellipticity of open clusters is rather uncertain, we determined King's parameters in Paper I assuming spherical symmetry in the projected distribution of cluster stars. Since we used integrated density profiles in the fitting routine, a possible bias due to a cluster flattening would be diminished. Indeed, in the outer cluster regions which are important for the tidal radius determination, the number of stars does not change, either when counted within a circle of radius R or within an ellipse with semi-major axis R. In the inner area of a cluster, a circle contains somewhat more stars than the corresponding ellipse. This would have a consequence for the determination of the core radius $r_{\rm c}$ but should not impact the results on the tidal radius $r_{\rm t}^{\rm m}$. On the other hand, the theoretical predictions propose a spherical form of cluster cores. Therefore, our approach should not lead to serious biases.

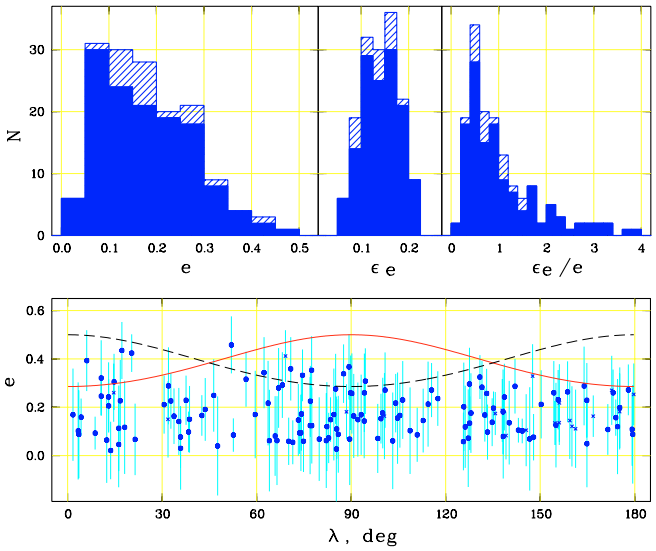

Fig. 2. Ellipticities of open clusters of our sample. *Upper panels*: distributions of ellipticities e, of their rms errors ε_e and relative errors ε_e/e. The hashed histograms are for clusters with at least 20 most probable members, the filled histograms show a subsample of these clusters at low Galactic latitudes ($|b| < 15°$). *Bottom panel*: distribution of observed ellipticity e versus aspect angle λ between the Solarcentric and Galactocentric vectors of a cluster. Dots are clusters with galactic latitude $|b| < 15°$, crosses are clusters at $|b| > 15°$. The bars indicate the rms errors. Curves give apparent ellipticities expected for open clusters at $|b| = 0°$ if they have a shape of a three-axial ellipsoid with an axis relation of 2:1.4:1 (solid curve) and of 1.4:2:1 (dashed curve). The first axis points towards the Galactic centre, the second axis in the direction of the Galactic rotation, the third one is perpendicular to the Galactic plane.

Using information on the membership of stars in the cluster areas, we determined ellipticities for clusters of our sample (Kharchenko et al. 2007). The ellipticity e is defined as

$$e = 1 - \frac{\mathcal{B}}{\mathcal{A}},$$

where $\mathcal{A}$ and $\mathcal{B}$ are semi-major and semi-minor axes of the apparent distribution of cluster members over the sky area. The semi-axes are computed as the principal axes of an ellipse using characteristic equations for the second-order moments of tangential coordinates of the 1σ cluster members.

In Fig. 2 (the upper panels) we give the distribution of ellipticities for clusters having at least 20 most probable members (i.e., 1σ-members). We conclude that the majority of these clusters have ellipticities smaller than 0.25, with an average of $\overline{e} = 0.18$ and a standard deviation of $\sigma_e = 0.10$. About 20% of clusters show a significant flattening ($\varepsilon_e/e < 0.5$), whereas for about 40%, the ellipticities do not significantly differ from zero ($\varepsilon_e/e > 1.0$). For clusters with tidal parameters determined in Paper I, the distribution of their ellipticities, rms errors, and relative errors have similar properties.

Strictly speaking, we should, however, consider the derived values of r_t^m to be lower limits of the tidal radii. Provided that a cluster has a form of a three-axial ellipsoid, we observe a projection rather than the real size of a cluster. The degree of possible discrepancy depends on the axis relation of the ellipsoid as well as on the orientations of the axes with respect to the line of sight to the cluster. According to Wielen (1985), due to the tidal coupling with the Milky Way, equipotential surfaces for an open cluster can be described by a three-axial ellipsoid. The orthogonal axes are related as 2:1.4:1, with the major axis directed towards the Galactic centre, the second axis oriented in the direction of Galactic rotation, and the third axis perpendicular to the Galactic plane. Provided that open clusters have this elongated form, we would underestimate the real tidal radii by a factor f of 1.4 at most, for clusters located in the Galactic plane at $l = 0°, 180°$. For all other clusters, the factor should be smaller and depends on the aspect angle λ' between the line of sight to the cluster (i.e. the Solarcentric vector) and its Galactocentric vector. Also, the projection of these ellipsoids on the sky must show a flattening depending on λ'. In Fig. 2 (bottom panel) we compare the observed distribution of ellipticities with the theoretical predictions based on Wielen (1985). For convenience we introduce an angle $\lambda = 180° - \lambda'$, so $\lambda = 0°$ at $l = 0°$, and $\lambda = 180°$ at $l = 180°$. Although several clusters have flattenings which coincide with the theoretical expectations, their distribution does not show a trend with λ. In general, the observed ellipticities are smaller than the predictions, and they are spread randomly around $e \approx 0.2$. We conclude that the majority of our clusters do not have a form of a three-axial ellipsoid, but are similar to oblate spheres with comparable axes towards the Galactic centre and along the Galactic rotation. Their real shape is probably defined by an interaction of different effects. This can result from a differential rotation of the Galaxy that would increase the second axis of the ellipsoids. Formally, open clusters with axis relations of 1.25:1.25:1 would show an ellipticity of 0.2 independent of λ. In the case of oblate spheres, the adopted method should not underestimate the tidal radii, since, even in a projection, we always see the largest axis. Therefore, we do not intend to correct our results for an ellipticity effect.

3.3. Distance dependent bias

Since our cluster sample is based on a magnitude limited survey (i.e. the ASCC-2.5 catalogue), one expects a different apparent structure of clusters located at different distances from the Sun due to a continuous loss of absolutely faint members in more remote clusters. This change of the apparent structure of a cluster with increasing distance can occur due to mass segregation i.e., due to a different concentration of members of different masses with respect to the cluster centre. In this context, "different input conditions" can cause a systematic bias in the resulting King parameters as a function of distances.

To estimate a possible distance dependent bias in the tidal radii determined, we carry out simulations based on a semi-empirical model of clusters of our sample. Starting from the original positions of a given cluster, we move, step by step, the cluster away (or move the observer away). At each step, its apparent structure changes since the cluster "shrinks", loses faint members, and its remaining members become fainter. In accordance with the standard rules of the pipeline that we applied in Paper I to determine tidal radii for our clusters, we build an apparent density profile of the "moved-away" cluster, fit the profile by the King model and compare the resulting tidal radius with the original finding.

3.3.1. The model

To take into account both the spatial and magnitude effects if a cluster is moved away, we developed a model based on stellar counts $\nu_{i,j}$ in radial and magnitude bins of $\Delta r = 0\overset{\circ}{.}05$ and $\Delta V = 1$ mag, respectively. In fact, these counts present the apparent luminosity functions $\phi(r, V)$ in radial circles.

For each cluster, the model considers two components: the "background", and the "cluster" populations. The background consists of field stars projected on the cluster area, the proper motions and photometry of which are compatible with those of the real cluster members. Such stars can occur even among the most probable cluster members. The density profile $\beta(r)$ of the background is computed in angular bins of r at the original position of the cluster and in the same way as that described in Paper I. In our model we assume that the background remains unchanged during the simulation, i.e. it does not depend on how far we move away a cluster.

The cluster component is obtained from counts $\nu_{i,j}$ inside the cluster area ($r \le r_2$) where r_2 is the observed radius of the cluster. The corresponding luminosity functions $\phi(r, V)$ are corrected for the background using a background luminosity function $\phi_\beta(V)$ constructed for the given cluster. Finally, the resulting luminosity functions in angular bins are converted to a linear scale in accordance with the distance of the cluster.

In the simulation, each cluster is moved away with steps of $\Delta(V - M_V) = 0.5$. At each step, magnitude bins dropping below the ASCC-2.5 limiting magnitude ($V_{\rm lim} = 13$) are excluded from further consideration, and a new density profile of the remaining cluster members is constructed from $\phi(r, V)$ integrated over the current magnitude range. Moving a cluster away makes it suffer from additional interstellar extinction. Interstellar extinction A_V was computed following Parenago's law

$$A_V = \frac{a_0\, h_z}{|\sin b|}\left(1 - \mathrm{e}^{-\frac{d|\sin b|}{h_z}}\right),$$

where $h_z = 100$ pc is the scale height of the Galactic disk dust layer, and $a_0 = A_V(\mathrm{COCD})/d(\mathrm{COCD})$ is the specific extinction in the cluster direction, calculated from the data available in the COCD. With this extinction approach we compute the corresponding distance to the cluster and convert the new density profile into an apparent distribution in angular bins. After adding the background component, we get a new observed density profile which is used in the pipeline for the determination of the tidal parameters. The calculations are stopped when the apparent radius of the cluster becomes smaller than 0.2 degrees, or the number of cluster members is less than 10 stars above the background level. These are the same limiting conditions as used in Paper I for the application of the pipeline.

3.3.2. Results

For 56 clusters of our sample, the model calculations were successful in at least 5 consecutive steps, i.e. these clusters could be moved away, totally, by more than $\Delta(V-M_V) = 2.5$. Their original distance moduli range from $(V-M_V) = 4.7$ to $(V-M_V) = 13$. The results of the simulations for these clusters are used to derive a correction to $r_{\rm t}^{\rm m}$ for a distance dependent bias.

In Fig. 3 we show density profiles of the Pleiades as would be measured in the ASCC-2.5 at two different distances of the cluster; at its real distance of 130 pc and at a distance of 530 pc from the Sun ($\Delta(V-M_V) = 3$ mag). This cluster is selected for illustrating the simulations since it has high quality membership, a long Main Sequence observed in the ASCC-2.5, and shows significant mass segregation (see Schilbach et al. 2006), i.e. the effect which may cause a distance dependent bias in the determination of the tidal radius. Moved to 530 pc, the Pleiades would have only about half of the members contained in the ASCC-2.5, and its apparent radius would be decreased by about a factor of four, from 6 deg to 1.5 deg. The distribution of members

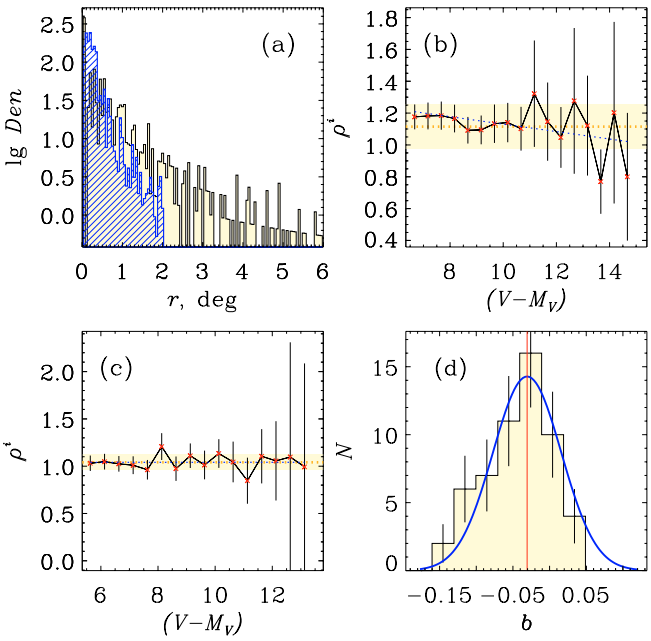

Fig. 3. Illustration of the performance of the simulation model. Panel **a)**: density profiles of the Pleiades apparent in the ASCC-2.5 at their original distance of 130 pc (filled histogram), and if they were moved to 530 pc (hatched histogram) from the Sun. r is the angular distance from the cluster centre. Panels **b)**, **c)**: relative variation of the tidal radius determined by the standard pipeline with increasing distance modulus; Panel **b)** – for α Persei. Panel **c)** – for the Pleiades. The dashed line is the average tidal radius, the dotted line shows the corresponding linear fit of data points. Panel **d)**: distribution of slope b for all 56 clusters included in the simulation. The solid curve reproduces the corresponding normal distribution.

appears to be more concentrated and sharper against the background. Though the accuracy of the tidal radius derived by the pipeline is lower with increasing distance due to poorer statistics, the changing of the conditions has only a small influence on its value (see Fig. 3, panel b). Nevertheless, for the majority of the 56 clusters the modelled tidal radii are decreasing with larger distances (e.g., see Fig. 3, panel d), though a few clusters obtain formally a positive gradient.

In order to quantify this effect, we consider a relative variation of the tidal radius $\rho^i = r_{\rm t}^i / r_{\rm t}^{\rm m}$ where $r_{\rm t}^{\rm m}$ is the tidal radius of a given cluster at its original distance, and $r_{\rm t}^i$ is its modelled value at a step i. For each cluster, an unweighted linear fitting of ρ is carried out as a function of $(V - M_V)$. The slope b of the resulting regression line gives the average relative variation of the tidal radius per step of $\Delta(V - M_V) = 0.5$. Since the use of "apparent distance modulus" already takes into account a value for A_V, the derived slope does not depend on the adopted details of the interstellar extinction. The distribution of b for all 56 clusters is shown in Fig. 3, panel (d). We conclude that our model calculations indicate a small but significant distant dependent bias in the determination of tidal radii, with an average slope of $\overline{b} = -0.031 \pm 0.006$ mag^{-1}. We checked whether the slope b computed from the model showed a dependence on cluster age, on a parameter s introduced in Schilbach et al. (2006) as an indicator of mass segregation, on the relation of the number of cluster members to background and on other parameters. A correlation was found only between b and $(V - M_V)$. In other words, if clusters are "moved away" the pipeline underestimates their tidal radii, and the degree of the underestimation is larger for remote clusters than for nearby ones.

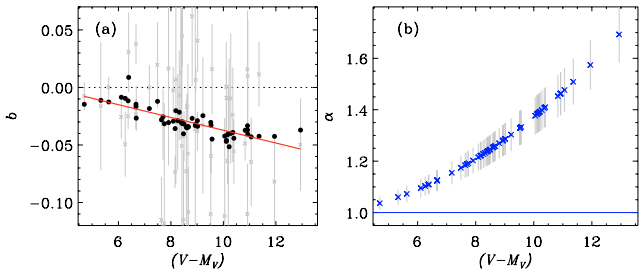

Fig. 4. Distance dependent bias in tidal radii. Panel **a)**: slopes of $\rho-(V-M_V)$ relation obtained by the model simulations for 56 clusters versus their original distance moduli. Crosses are original slopes, squares are smoothed points after applying a Lee filter. The corresponding least squares fit is shown by a dotted line. Panel **b)**: correction factor versus distance modulus. This correction is applied to the cluster tidal radii determined by the standard pipeline, to remove a distance dependent bias in the results.

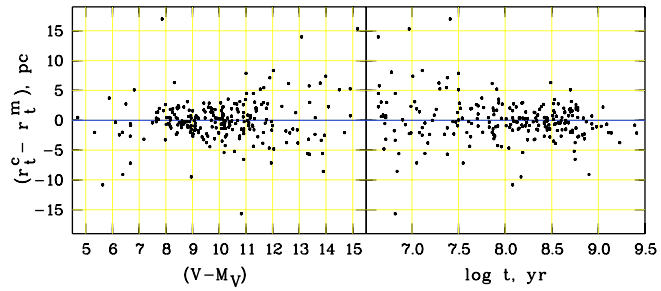

Fig. 5. Differences between measured and calibrated tidal radii via distance modul (*left*) and age (*right*) of 236 open clusters of our sample.

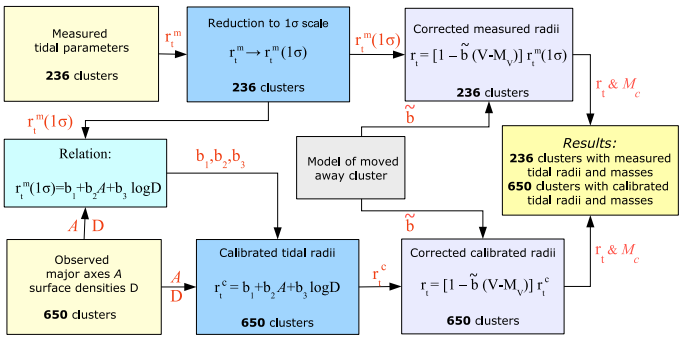

Fig. 6. Schema of construction of the uniform scale of tidal radii.

In Fig. 4a we show the distribution of model slopes b versus original distance modulus. Since individual data points b have relatively large rms errors, and their scattering is relatively large, too, we apply a Lee filter (a standard statistical filtering routine of the IDL library) which is recommended for retrieving a systematic trend in "noisy" data. The distribution of smoothed points can be well approximated by a linear polynom

$$\tilde{b} = (0.0184 \pm 0.0048) - (0.0056 \pm 0.0005) \times (V - M_V).$$

The corresponding correction factor $\alpha = r_t/r_t^m$ is computed as

$$\alpha = 1 - \tilde{b} \times (V - M_V) \qquad (1)$$

where r_t^m is the tidal radius of a cluster obtained with the original pipeline and presented in Paper I, and r_t is the tidal radius corrected for a distant dependent bias of the procedure applied. It gives the value that a cluster would have if it were located at 10 pc from the Sun (i.e. at $(V - M_V) = 0$). The dependence of the correction factor α on the distance modulus of a cluster is shown in Fig. 4b. Since the majority of our clusters are located at $(V - M_V) < 11$, their previously published tidal radii r_t^m were, consequently, underestimated by a factor less than 1.5 (from $\alpha = 1.008$ for Mel 111 at 87 pc from the Sun to 1.467 for NGC 2539 at ≈1.3 kpc). For the most remote clusters of our sample ($(V - M_V) = 15$ at 3 kpc...6 kpc), α gets about 2. However, for clusters with $(V - M_V) > 13$ the correction factor α should be considered with caution since it is based on an extrapolation of Eq. (1) derived with clusters at $(V - M_V) < 13$.

The coefficient α is used in Sect. 4 to correct the previous tidal radii for the distant depending bias estimated here.

4. Building the homogeneous system of tidal parameters

Tidal parameters were determined by a direct fitting of the King model to the observed density distribution of cluster members (see Paper I) for 236 (36%) of our clusters. In order to obtain a more significant basis for a further analysis of the cluster population, an estimation of cluster masses is desirable for the remaining 414 clusters. Therefore, we searched for a calibration that can be used to derive cluster tidal radii from observed parameters available for each cluster. As possible candidates, one can consider the linear radius r_2 or the semi-major axis $\mathcal{A}$ (see Sect. 3.2) since they both describe the structure of a cluster, though in different way.

Being a second-order moment, $\mathcal{A}$ is related to the internal density distribution of cluster members within a cluster, whereas r_2 is defined as a maximum apparent distance of cluster members from the cluster centre. From this aspect, r_2 is more consistent with a tidal radius. On the other hand, from a statistical point of view, $\mathcal{A}$ is a more robust estimate than r_2 since it is based on information on all cluster members. As this property is an important factor for the determination of tidal masses of clusters, we decided to make the calibration rely upon $\mathcal{A}$. For a better agreement between the systems of tidal radii r_t^m and of second-order moments $\mathcal{A}$, we include a term depending on the surface density of cluster members in the reduction polynomial. The best least-squares fit of $\mathcal{A}$ to r_t^m is achieved with the relation

$$r_t^m = b_1 + b_2\,\mathcal{A} + b_3\,\log D_n, \qquad (2)$$

where $b_1 = 1.12 \pm 0.23$ pc, $b_2 = 3.45 \pm 0.09$, $b_3 = 2.45 \pm 0.41$ pc, and D_n is the surface density of 1σ-members within r_2 in a given cluster. In Fig. 5 we show the differences between measured and calibrated values of tidal radii of 236 clusters versus distance modulus $(V-M_V)$ and age of these clusters. Though differences have a larger scattering for younger and/or distant clusters, they do not show significant dependence on the distance modulus and the age of clusters. We use the empirical relation (2) to estimate the tidal radii r_t^c of all 650 clusters.

The complete scheme of data reduction is shown in Fig. 6. We start with 236 clusters having tidal parameters r_t^m determined directly from the fitting of three-parametric King's profiles to the observed integrated density distribution of cluster members. For clusters with tidal radii based on the solutions with 2σ-, 3σ-, or "4σ"-membership groups, we apply the relations derived in Sect. 3.1 and convert them into the system defined by 1σ-members. The resulting $r_t^m(1\sigma)$ of 236 clusters are used to find a relation between tidal radius and semi-major axis $\mathcal{A}$ which is also, obtained from the distribution of 1σ-members. Then, this relation is used to estimate calibrated tidal radii r_t^c for all clusters of our sample. In the next step, we correct $r_t^m(1\sigma)$ and r_t^c for the

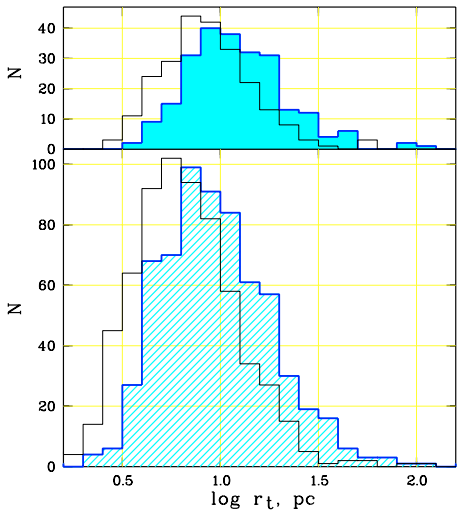

Fig. 7. Distributions of tidal radii. The upper panel shows the measured radii for 236 clusters. In the lower panel the distribution of calibrated radii is given for all 650 clusters of our sample. The open histograms correspond to uncorrected radii, the filled/hatched ones are for radii corrected for biases.

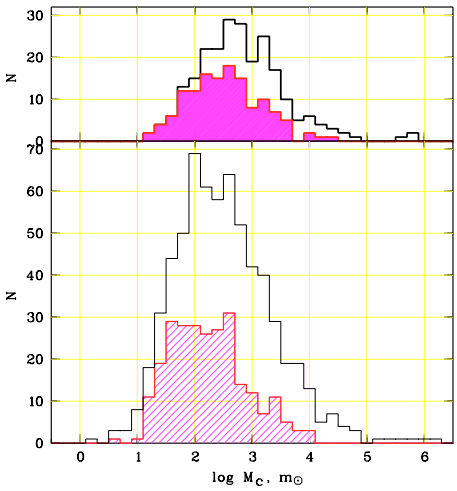

Fig. 8. Distributions of tidal masses of open clusters. The upper panel shows masses calculated from measured radii for 236 clusters. The lower panel displays the masses calculated from calibrated radii of all 650 clusters of our sample. The open histograms correspond to total distributions, the filled/hatched ones are distributions of corresponding clusters residing in the area where our sample is complete.

distance dependent bias as found in Sect. 3.3. Finally, according to King (1962), the resulting tidal radii r_t are used to compute tidal masses M_c for each of the 650 clusters from

$$M_c = \frac{4\,A\,(A-B)\,r_t^3}{G}, \qquad (3)$$

where A, B are Oort's constants valid at the galactocentric distance of the cluster, and G is the gravitational constant (see Standish 1995).

5. Results and comparison with counted masses

The tidal radii and masses for the clusters of our sample are listed in a table that is available in electronic form only, and can be retrieved from the CDS. For each of the 650 open clusters we give, among other relevant data, the tidal radius and the corresponding mass computed from the semi-major axis $\mathcal{A}$ as described above (i.e. calibrated parameters). For 236 clusters, the table also contains the tidal radii and masses based on the direct fitting of the King model (i.e. measured parameters). The measured parameters should have a higher priority if the reader is interested in studying individual clusters. For stellar statistical investigations, however, calibrated parameters are better suited since they are more homogeneous and available for a larger sample that is complete up to a distance of about 850 pc from the Sun (see Piskunov et al. 2006). All (measured and calibrated) tidal parameters are corrected for the distance dependent bias. The median precision of the tidal radii is about 2 pc, and the median of their relative errors is 0.22.

In Fig. 7 we compare measured (upper panels) and calibrated (bottom panels) tidal radii before and after the correction for a distance depending bias (open and filled histograms, respectively). As expected, the corrected radii are, on average, larger, but the shape of their distributions remains the same as before the corrections. Also, the distributions of measured and calibrated tidal radii do not differ significantly. Although the sample of calibrated radii has a larger proportion of small clusters ($r_t < 8$ pc), their distribution fits naturally to the distribution of measured tidal radii, and it does not show any features that would suggest some biases.

We come to a similar conclusion if we consider the distribution of the corresponding tidal masses in Fig. 8: the distribution of calibrated masses (open histogram, lower panel) suits well the distribution of measured tidal masses (open histogram, upper panel). As expected, the subsample with measured data includes a larger fraction of the clusters at distances less than 850 pc from the Sun where our cluster sample was found to be complete. A typical cluster without measured but with calibrated mass is either located at a larger distance, or it is nearby but is a poorly populated cluster like NGC 7058, King 6, Mamajek 1. The wing of the mass distribution at $\log M_c > 5$ consists exclusively of associations.

In Paper I we compared our original results on tidal masses with independent determinations based on stellar counts taken from the literature. We found some discrepancies that could not be explained conclusively. Now, after correcting our preliminary results for different systematic effects, it makes sense to repeat the comparison.

We consider masses of galactic open clusters given in Tadross et al. (2002), Danilov & Seleznev (1994), and Lamers et al. (2005). Tadross et al. (2002) derived cluster masses M_T for 160 clusters from direct counts of cluster members on CCD frames. Their results are based on published data taken from different sources. Using original observations, Danilov & Seleznev (1994) determined masses M_D for 103 compact, distant (>1 kpc) clusters by counting stars in cluster areas. Where necessary, the Salpeter IMF was applied to extrapolate the counts to the limiting magnitude $B = 16$. Lamers et al. (2005) used data of the COCD to get a normalization of the Salpeter IMF. The masses M_L were derived for about 380 clusters by extrapolation of the normalized Salpeter IMF to low mass stars down to 0.15 $m_\odot$. In Paper I we found that our preliminary results on tidal masses are comparable with M_T and M_D but are considerably lower than M_L. Since M_T and M_D were expected to be smaller tidal masses, we did not exclude the possibility that our results were underestimated. On the other hand, the lower limit of mass integration was chosen arbitrarily in Lamers et al. (2005), and this (according to Lamers 2007) could cause a mass overestimation by a factor of two or three. As the masses in

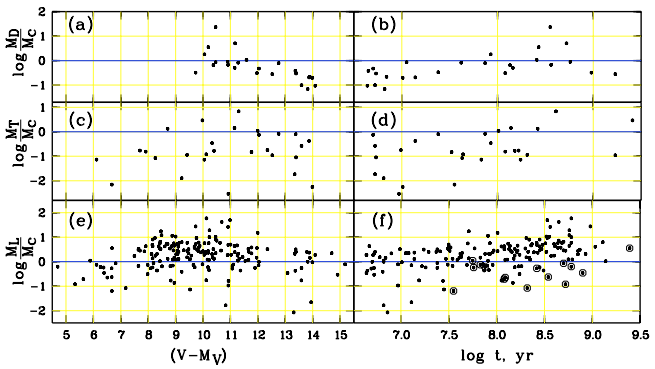

Fig. 9. Comparison of measured tidal masses M_c corrected for the distant dependent bias with published data on counted- and MF-scaled masses. Ratios are presented as functions of the distance modulus (*left panels*) and cluster age (*right panels*). The published masses M_D are taken from Danilov & Seleznev (1994) (panels **a)** and **b)**), M_T from Tadross et al. (2002) (panels **c)** and **d)**), and M_L from Lamers et al. (2005) (panels **e)** and **f)**). Clusters at $(V - M_V) < 7.5$ are marked by open circles in panel **f)**.

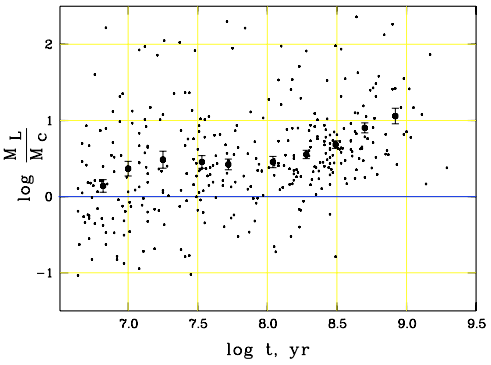

Fig. 10. Same as Fig. 9f but for calibrated tidal masses M_c of clusters at $(V - M_V) > 7.5$. Large filled circles with error bars indicate a running average of $\log M_L/M_c$ with a $(\log t)$-bin of 0.5 and a step of 0.25.

Lamers et al. (2005) and Paper I are based on the same data on membership and cluster parameters taken from Kharchenko et al. (2004) and Kharchenko et al. (2005a) but use different methods of mass determination, the disagreement calls for a clear explanation. This was one of the main reasons for us to consider possible biases in our tidal parameters more carefully.

In Fig. 9 we compare the cluster masses quoted above with tidal masses computed from the corrected tidal radii. As expected, M_T and M_D are, on average, smaller than the tidal masses. The trend in Fig. 9a can be attributed to the data of Danilov & Seleznev (1994), and it can be explained by a constant limit of apparent magnitudes used for star counts in all clusters independent of their distance from the Sun.

On average, the differences between our tidal masses and M_L have decreased compared to Paper I, though they are still too large to be explained by random uncertainties of the methods. According to Fig. 9e, one can separate three groups of clusters: clusters at $(V - M_V) < 7.5$ with M_L smaller by a factor of 2.5 than the corresponding tidal masses, clusters at $7.5 < (V - M_V) < 12$ where M_L are, on average, three times larger than tidal masses, and clusters at $(V - M_V) > 12$ where both mass estimates are in reasonable agreement (except two associations with $13 < (V - M_V) < 14$). We believe that the disagreement in masses of nearby clusters has a different nature than the mass disagreement of more distant clusters.

For nearby clusters, the discrepancy can be explained by a low normalization factor used by Lamers et al. (2005) for the construction of cluster IMFs. This bias may arise from a dependence of the completeness limit of the ASCC-2.5 on $(B - V)$ of the stars. On average, the ASCC-2.5 is complete to $V = 11.5$ for A or F stars. For later spectral classes, the completeness limit becomes brighter than $V = 11.5$. Therefore, in a cluster area with a given nearby cluster, the ASCC-2.5 may contain field stars down to $V = 11.5$ but the faint (i.e., red) cluster members in the flatter part of the cluster main sequence would be missing. If a normalization is computed for the whole magnitude range down to $V = 11.5$ but with an incomplete sample of cluster members at the faint end, the corresponding factor will be too low. In more distant clusters, ASCC-2.5 contains only members in the steeper part of the main sequence, i.e., cluster stars with smaller $(B-V)$. Therefore, the completeness limit of the ASCC-2.5 corresponds to the completeness limit of cluster members, and the normalization factors for the IMFs become correct for remote clusters.

For clusters at $(V - M_V) > 7.5$, the reason for the disagreement between M_L and tidal masses is completely different. As we have shown in Schilbach et al. (2006), our sample contains clusters of different ages at $(V-M_V) < 10.5$, and with increasing distance the sample becomes more and more "young" since, at large distances, the ASCC-2.5 contains only blue luminous stars which are only present in young clusters. This is a natural consequence of each magnitude-limited survey used for cluster identification. The systematic effect apparent in Fig. 9e can, therefore, be better understood if we consider the relation M_L/M_c as a function of cluster age (Fig. 9f). The cluster population within 1 kpc from the Sun includes a large portion of clusters with typical ages of several hundred Myrs (Piskunov et al. 2006). In such clusters, due to a loss of members (preferentially of small masses) during the dynamical evolution (e.g. Baumgardt & Makino 2003), the mass spectra of cluster members differ from the initial mass functions. Assuming the Salpeter IMF for these clusters, one would, therefore, overestimate cluster masses. This can explain the increasing difference between M_L and tidal masses with increasing age of clusters. Note that nearby clusters follow the same general trend in Fig. 9f like the more distant clusters.

This conclusion has statistical support in Fig. 10 where we compare calibrated tidal masses with data of Lamers et al. (2005). We exclude associations and nearby clusters at $(V - M_V) < 7.5$ from the consideration. Since calibrated tidal masses are available for all clusters, the number of data points is, however, about twice as large as in Fig. 9f. We conclude that both mass estimates are in reasonable agreement for the youngest clusters where dynamical evolution had no time to change the IMF significantly. For clusters with ages $7.25 < \log t < 8$ (a typical scale for two body encounters), the ratio M_L/M_c does not change much but is significantly larger than 1. This can indicate that, already in relatively young clusters, the actual mass function differs from the Salpeter IMF. For clusters of larger ages the ratio M_L/M_c steadily increases with time and reaches a factor of 10 for the oldest clusters. We interpret the systematic trend in Fig. 10 as indirect evidence from observations of an evolution of MFs in open clusters.

6. Summary and conclusions

Although being a basic parameter in studies of cluster evolution, the mass of an open cluster can not be derived directly from the

present day observations. Indirect methods require, however, a number of assumptions that can cause different biases in the resulting mass estimates. In Paper I we presented mass estimates of 236 clusters derived via tidal radii. The tidal radii were obtained from a three-parameter fit of King's profiles to the density distribution of cluster members projected on the sky. This method assumes systems with spherical density distributions whereas open clusters can have elliptical shape and a preferential orientation of their main axes in the Galaxy. In this case one should expect a systematic underestimation of tidal radii, depending on the location of clusters with respect to the Sun and to the centre of the Galaxy. Though a typical open cluster shows an ellipticity (for details see Kharchenko et al. 2007), no significant trend is found depending on the aspect angle of clusters. Therefore, we assume that the orientation of open clusters is rather random. Moreover, the average ellipticity is relatively small ($\overline{e} = 0.18 \pm 0.10$) in order to produce a prominent bias in the determination of tidal radii. We cannot claim that for individual clusters the ellipticity would not have an impact on the results, however this will not affect the general conclusions based on statistical studies on the cluster population.

Another possible bias in the resulting tidal radii may arise from the relative bright magnitude limit of the ASCC-2.5 that was used to identify the clusters, to determine the membership and to construct the density profiles in cluster areas. Beyond 300 pc from the Sun, the ASCC-2.5 practically does not include dwarfs later than G0. This fact can introduce discrepancies in the determination of tidal radii by the method applied. The question is whether possible discrepancies are of systematic or random nature. Taking into account apparent luminosity functions of cluster members and field stars in each cluster area, we constructed a semi-empirical model of clusters found in the ASCC-2.5. "Moving" a cluster away from the Sun, we applied the standard pipeline for the determination of tidal radii. We found that, on average, the pipeline produces smaller tidal radii with increasing distance of the clusters: for nearby clusters the correction factor is almost 1 but it becomes about 1.7 for clusters at $(V - M_V) = 13$. As the simulations are limited to clusters with $(V - M_V) \leq 13$, for more distant clusters the correction factor is the result of an extrapolation reaching a value of about 2 for the most distant cluster of our sample at $(V - M_V) \approx 16$.

Unfortunately, the subsample of 236 clusters with tidal radii derived from the King model is neither representative nor complete to a given distance from the Sun. Therefore, the other main goal of this work was to find a parameter available for all clusters of the sample to estimate the cluster tidal radii. Among different candidates we chose the semi-major axis of the projected distribution of cluster members within the cluster area. The relation between tidal radii and the semi-major axis of 236 clusters was then used to compute calibrated tidal radii for all 650 clusters. We did not find systematic differences between measured and calibrated tidal radii as a function of cluster distance or age. Again, for individual clusters the relation may not be perfect but using reliable information on cluster membership, it provides a confident basis for statistical studies of the properties of the local cluster population.

After the correction for a distance depending bias, measured and calibrated tidal radii were used to derive tidal masses for the clusters. As expected, tidal masses are, on average, larger than masses obtained exclusively from star counts by Danilov & Seleznev (1994) and Tadross et al. (2002). On the other hand, we find systematic differences between tidal masses and mass estimates by Lamers et al. (2005) who used COCD data on star counts and the Salpeter IMF extrapolated down to $m = 0.15\ m_\odot$. The discrepancy is small for young clusters and increases considerably with cluster age. We believe that the systematics can be reduced if the mass estimates by Lamers et al. (2005) would consider a change of the mass function of a cluster during its dynamical evolution. This assumption can be verified by comparison with virial masses of open clusters that are based on another independent method of mass estimate. A corresponding project is underway (Gieles 2007).

Acknowledgements. We acknowledge the anonymous referee for his/her comments, which enabled us to improve the clarity of the paper. This study was supported by DFG grant 436 RUS 113/757/0-2, and RFBR grant 06-02-16379.

References

Adams, J. D., Stauffer, J. R., Monet, D. G., Skrutskie, M. F., & Beichman, C. A. 2001, AJ, 121, 2053
Adams, J. D., Stauffer, J. R., Skrutskie, M. F., et al. 2002, AJ, 124, 1570
Baumgardt, H., & Makino, J. 2003, MNRAS, 340, 227
Chen, W. P., Chen, C. W., & Shu, C. G. 2004, AJ, 128, 2306
Danilov, V. M., & Seleznev, A. F. 1994, Astron. Astrophys. Trans., 6, 85
Gieles, M. 2007, private communication
Gieles, M., Portegies Zwart, S., Baungardt, H., et al. 2006, MNRAS, 371, 793
Gieseking, F. 1981, A&A, 99, 155
Kharchenko, N. V. 2001, Kin. Phys. Celest. Bodies, 17, 409
Kharchenko, N. V., Piskunov, A. E., Röser, S., Schilbach, E., & Scholz, R.-D. 2004, Astron. Nachr., 325, 743
Kharchenko, N. V., Piskunov, A. E., Röser, S., Schilbach, E., & Scholz, R.-D. 2005a, A&A, 438, 1163
Kharchenko, N. V., Piskunov, A. E., Röser, S., Schilbach, E., & Scholz, R.-D. 2005b, A&A, 440, 403
Kharchenko, N. V., Piskunov, A. E., Berczik, P., et al. 2007, A&A, in preparation
King, I. 1962, AJ, 67, 471
Lamers, H. J. G. L. M. 2007, private communication
Lamers, H. J. G. L. M., Gieles, M., Bastian, N., et al. 2005, A&A, 441, 117
Oort, J. 1979, A&A, 78, 312
Piskunov, A. E., Kharchenko, N. V., Röser, S., Schilbach, E., & Scholz, R.-D. 2006, A&A, 445, 545
Piskunov, A. E., Schilbach, E., Kharchenko, N. V., Röser, S., & Scholz, R.-D. 2007, A&A, 468, 151
Raboud, D., & Mermilliod, J.-C. 1998a, A&A, 329, 101
Raboud, D., & Mermilliod, J.-C. 1998b, A&A, 333, 897
Schilbach, E., Kharchenko, N. V., Piskunov, A. E., Röser, S., & Scholz, R.-D. 2006, A&A, 456, 523
Standish, E. M. 1995, in Highlights of Astronomy
Tadross, A. L., Werner, P., Osman, A., & Marie, M. 2002, NewA, 7, 553
Wielen, R. 1974, in Proceedings of the 1st European Astronomical Meeting, Stars in the Milky Way system, 2, 326
Wielen, R. 1985, in Dynamics of star clusters, ed. J. Goodman, & P. Hut (Dordrecht: D. Reidel Publishing Co.), 449